华北北部中元古界洪水庄组物源和沉积环境分析

马奎[1],肖南[2],蒲钰龙[3],钟佳倚[1]

(1.中国石油西南油气田公司勘探开发研究院,四川 成都 610041;2.重庆市地质矿产勘查开发局208水文地质工程地质队,
重庆 400700;3.中国石油新疆油田分公司采油一厂,新疆 克拉玛依 834000)

提要:为探讨华北地区中元古界洪水庄组黑色泥页岩物源和沉积环境,采集了燕辽地区清河剖面洪水庄组样品,进行元素地球化学测试和分析。结果表明:洪水庄组沉积物来源不仅有陆源碎屑物质,还有海水沉积物贡献。Y/Ho和ΣREE交会图版分析认为海水沉积物来源占比为10%~20%。此外,稀土元素分布模式以及Ce和Eu异常表明沉积物来源有火山热液活动的参与。Mo-EF/U-EF分析结果表明洪水庄为海洋非滞留海盆沉积环境,氧化还原条件在沉积期发生了演变:在洪一段沉积时期,水体还原程度强,为厌氧-硫化环境;洪二段沉积时期,水体还原程度降低,为贫氧-厌氧环境。分析认为洪水庄组物源组成和沉积环境演变与沉积构造背景密切相关。

关　键　词:中元古界;洪水庄组;泥页岩;沉积环境;物源;油气地质调查工程;华北北部

中图分类号:P588.2;P534.3　　　文献标志码:A　　　文章编号:1000−3657(2021)01−0309−13

Provenance and sedimentary environment of the Mesoproterozoic Honghongzhuang Formation in northern part of North China

MA Kui[1], XIAO Nan[2], PU Yulong[3], ZHONG Jiayi[1]

(1.PetroChina Southwest Oil & Gas Field Company, Chengdu, 610041, Sichuan China;2. Hydrogeology and Engineering Geology Team of Chongqing Bureau of Geology and Minerals Exploration, Beibei District, Chongqing 400700, China;3. PetroChina Xinjiang Oilfield Company No.1 Oil Production Plant, Karamay, 834000, Xinjiang China)

Abstracts: In order to further explore the provenance and sedimentatary environment of mud shale in the Mesoproterozoic Hongshuizhuang Formation of northern China, samples were collected from outcrops of the Qinghe section of Honghongzhuang Formation for elementary geochemical testing and analysis. The results show that the sediments were not only from terrigenous clastics but also from marine sediments. The results of Y/Ho and ΣREE relationship diagram analysis show that the source proportion of seawater sediments is 10%−20%. In addition, the distribution pattern of rare earth elements and the Ce and Eu anomalies indicate the involvement of volcanic hydrothermal activity in the sediment source. Mo−EF /U−EF analysis results show that Hongshuizhuang is a sedimentary environment of Marine non−stationary basin, and the evolution of redox conditions in the

sedimentary period is as follows: in the period of the Lower Member deposition of Hongshuizhuang Formation, the water body was in a strong reductive anaerobic−sulfurization environment; while, during the period of its Upper Member deposition, the reduction degree of water decreased and the environment was anaerobic. It is concluded that the provenance composition and sedimentary environment evolution of the Honghongzhuang Formation are closely related to the sedimentary tectonic setting.

1 引 言

华北燕辽地区中新元古界发育有多套优质烃源岩,油气资源潜力巨大,具有良好的勘探前景。蓟县系洪水庄组泥页岩就是中国大陆最古老的烃源岩之一,有机质丰度高,沉积连续且分布稳定(郝石生等, 1990; 王铁冠和韩克猷,2011)。前人关于洪水庄组的研究主要包括生烃潜力评价(王杰和陈践发, 2001; 方杰等, 2002; Liet al., 2003),结合岩性、岩相对沉积环境进行判别(霍勇等, 2012;罗顺社等, 2012),以及探讨了古生产力与有机质富集的关系(罗情勇等, 2013)。而关于该套黑色页岩形成的沉积环境、物源研究工作较为薄弱。

由于洪水庄组有机质成熟度低,岩性以泥页岩为主,其化学组成基本保存了物源的原始信息,能够更真实的反映物源组成和原始沉积环境。而对华北北部中元古界黑色岩系的沉积环境和物源研究,一方面对于探讨多类矿床的成因具有重要的意义(孙省利等, 2003;陈践发和孙省利, 2004);另一方面,对于中国元古宇油气资源评价与勘探开发更具有重要的理论与实际意义(吴因业等, 2016;赵文智等, 2018)。因此,本研究通过采集华北北部宽城地区洪水庄组不同岩性的岩石样品,以研究物源组成和沉积环境恢复为目的,开展元素地球化学方面分析工作,为华北燕辽地区中元古代沉积环境的重建提供理论支撑,并为元古宇古老含油气系统的有效性评价和勘探潜力研究奠定基础。

2 区域地质背景

华北克拉通北部燕辽裂陷带发育系统完整的中新元古界,其沉降史稳定,热演化史温和,经历了3个阶段的构造演化阶段:早期发生阶段(1800~1600 Ma)、中期发展阶段(1600~1400 Ma)和晚期消亡阶段(1400~1300 Ma)(秦婧, 2010)。洪水庄组沉积处于燕山裂陷带形成的晚期(乔秀夫和高林志, 2007;李怀坤等, 2010)。其沉降中心主要分布在蓟县、兴隆和宽城一带,地层厚度分布稳定,为100~170 m。西部地层厚度较薄(如宣龙坳陷怀来赵家山剖面,约100 m),东部地层厚度厚(如冀北坳陷宽城至辽西坳陷凌源一带,约170 m)。宽城一带岩性最为典型,岩性自下而上可分为泥页岩段和白云岩段,泥页岩段主要包括硅质页岩、页岩和泥岩,白云岩段包括泥晶白云岩和白云质泥岩(图1)。其中,硅质页岩段颜色为灰黑色、呈薄层状,与黑灰色白云质泥岩不等厚互层,属于较稳定的潮下带沉积,主要分布在洪水庄组底部(图2a)。实测剖面厚度为12.5 m,占总厚度的9.7%。页岩和泥岩多为灰黑色、黑色(图2b),局部见泥灰岩透镜体,页理极为发育,为水浅海沉积环境。实测剖面厚度为72.7 m,占总厚度的55.7%,是洪水庄组主要的岩石类型。白云质泥岩主要发育在洪水庄组顶部,夹杂薄层的泥晶白云岩,为潮下带沉积。实测剖面厚度为45 m,占地层总厚度的34.6%。

3 样品采集与分析测试

样品采集地点位于河北省承德市宽城县清河剖面(地理坐标：40°32'38" N, 118°14'58" E),该剖面发育完整的洪水庄组地层,经过测量,剖面总厚度为130 m(图3)。从老到新依次收集不同岩性样品共29件,在采集样品过程中尽可能采集未经风化的新鲜岩样。采样间距有所不同,重点采集泥页岩类样品,其中白云质泥岩样品8件,泥岩样品4件,
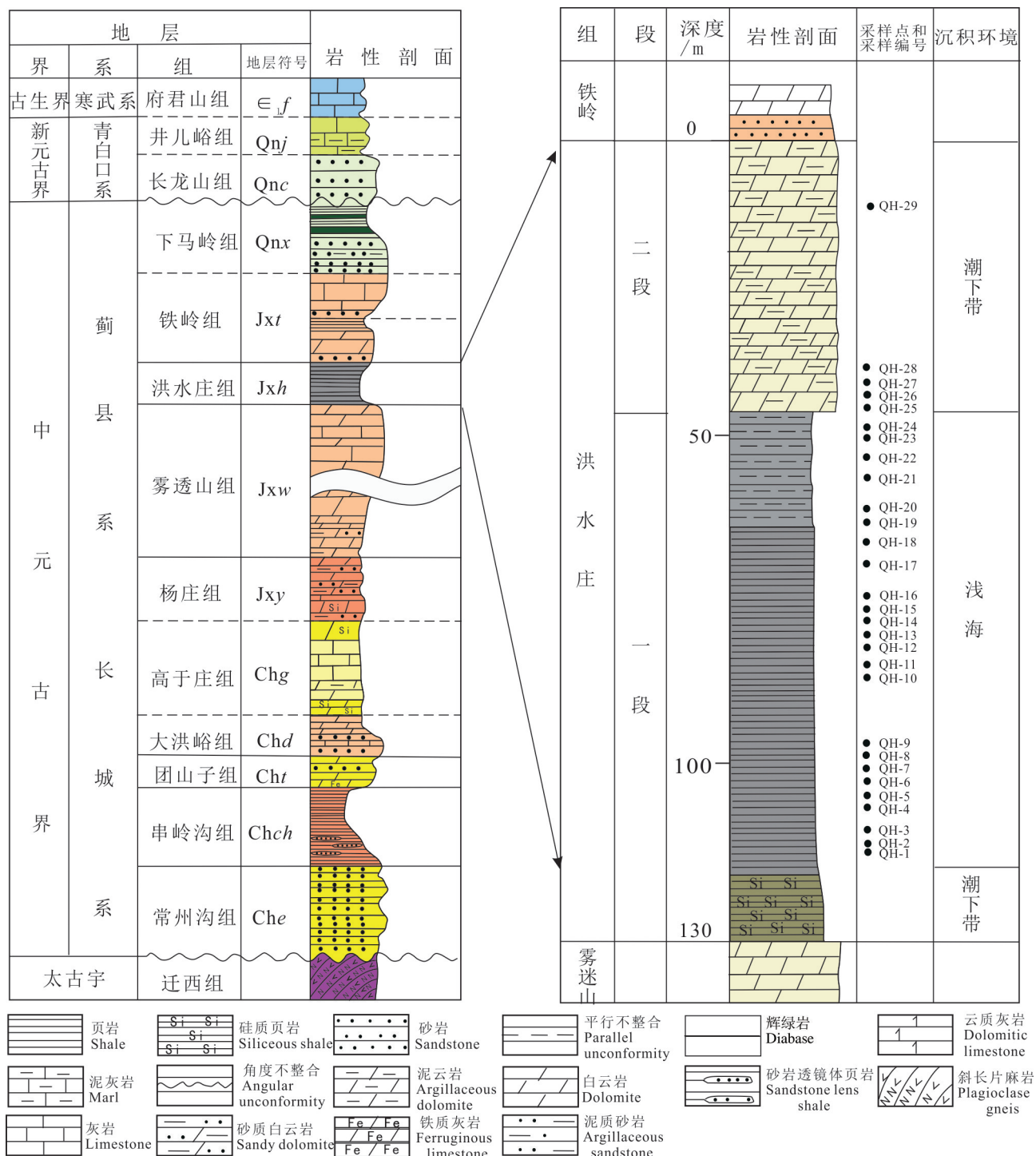
图1 华北北部燕山地区中新元古界地层柱状图(左)和清河剖面洪水庄组岩性柱状图(右)

Fig.1 The Mesoproterozoic−Neoproterozoic stratigraphic column of the Yanshan area (left) and lithological columns of the Hongshuangzhuang Formation of the Qinghe section(right) in north China

页岩样品14件,泥质硅质泥岩3件(图1)。

元素分析:样品的前处理和样品元素分析均在北京核工业地质研究院进行。分析步骤如下:将采集的样品经过去风化处理,粉碎至200目以下,然后装袋备用。称取50 mg样品于封闭容样装置中,加入1 mL HF放在电热板上蒸干去掉大部分的SiO_2。
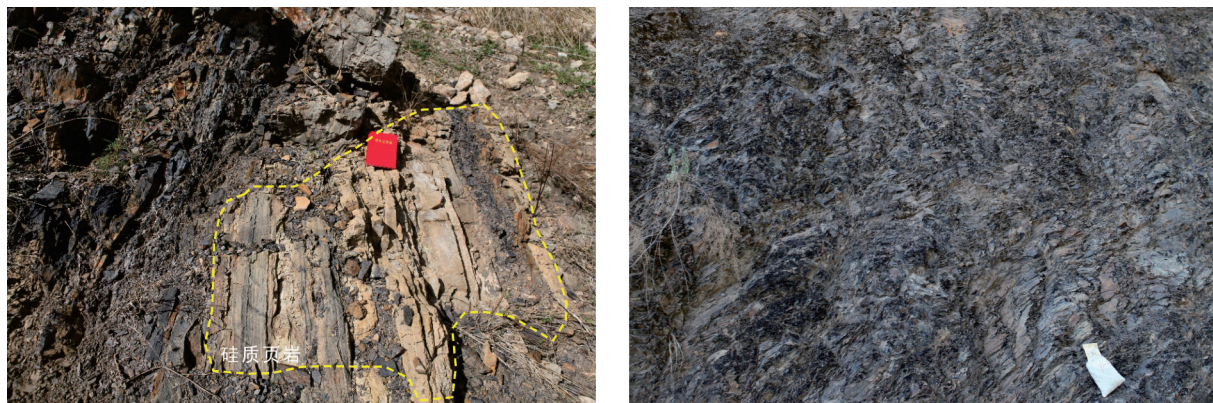
图2 华北宽城清河剖面洪水庄组野外露头(a−硅质页岩;b−灰黑色泥页岩)

Fig.2 Outcrop of the Hongshuizhuang Formation in the Qinghe section, Kuancheng, North China (a−siliceous shale; b−grayish black shale)

再加入 1 mLHF 和 0.5 mLHNO₃ 再蒸干,置于电热箱中并升温至 200℃ ,加热约 48 h。 最后加入 2 mLHNO₃ 和 5 mL 水,重新盖上盖,于 130℃ 溶解残渣 3 h,加入 Rh 和 Re 作为内标,转移至 50 mL 离心管中,待上仪器测定。国家标准物质 GB7107(页岩) 和 GB7114(白云岩)用于控制分析精度。采用仪器为 ICAP9000N+1 等离子光量计,其波长范围为 190~ 900 nm,分辨率为 0.036 nm(一级),检测限为 10⁻⁹级,分析精度由于 5%。

4 测试结果

微量元素:对 Co、Mo、V、Cr、Ni、U、Th、和 Cu 等 8 种微量元素进行测试(表1,图4a)。其中 V 元素含量较高,为 43×10⁻⁶~487×10⁻⁶,平均266.58×10⁻⁶。其他微量元素含量相对较少,Zr 为 42.5×10⁻⁶~146×10⁻⁶,平均110.2×10⁻⁶;Cr 为 35.1×10⁻⁶~84.1×10⁻⁶,平均59.6×10⁻⁶;Ni 为 12.2×10⁻⁶~85.5 ×10⁻⁶,平均41.3 ×10⁻⁶。Mo、Th、Sc、Co 含量最少,Mo 为 0.32×10⁻⁶~43.4×10⁻⁶,
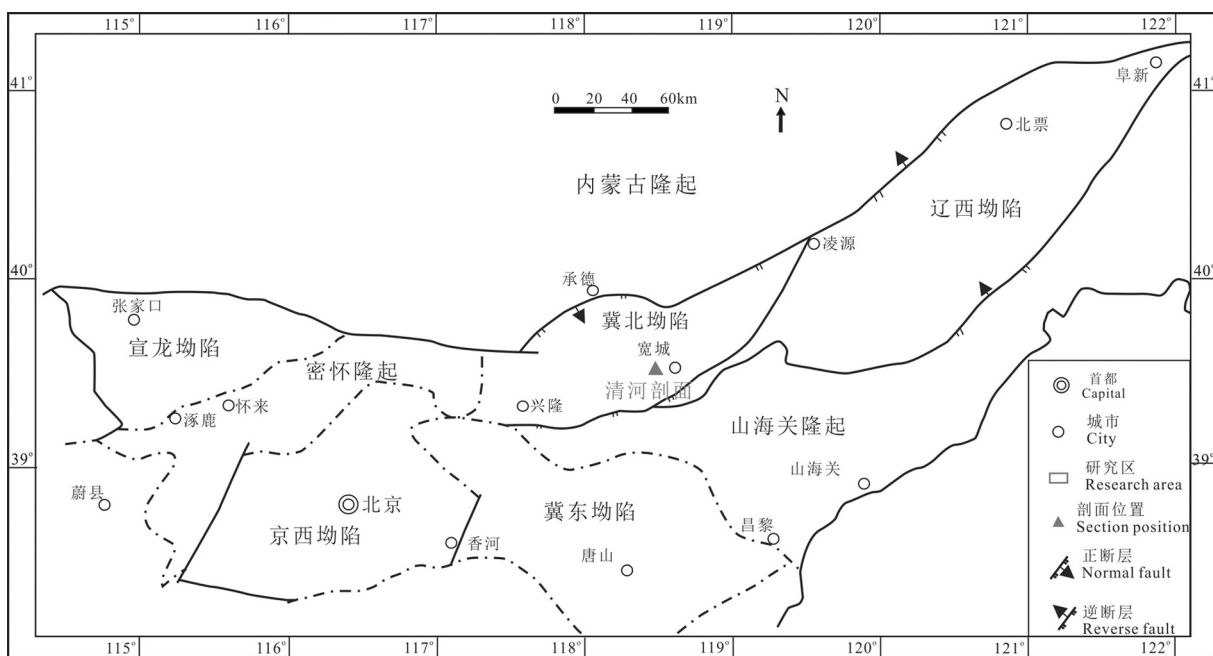

图3 华北北部燕辽裂陷现今构造区划简图

Fig.3 Simplified map of geological structure in Yanshan area of north China

表1 华北北部中元古界清河剖面洪水庄组样品微量元素含量(10⁻⁶)

Table 1 Contents (10⁻⁶) of trace elements in the samples of Hongshuizhuang Formation from Qinghe section of Middle Proterozoic in north China

样品	岩性	Mo	U	Th	V	Cr	Ni	Co	La	Ce	Pr	Nd	Sm	Eu	Gd	Tb	Dy	Ho	Er	Tm	Yb	Lu	Y
QH-1	硅质泥岩	1.8	2.7	6.27	125.0	46.5	20.0	1.12	19.4	42	5.65	23.9	4.9	0.89	4.11	0.756	4.15	0.746	2.16	0.311	2.11	0.344	24.2
QH-2	硅质泥岩	9.2	5.8	6.73	264.0	51.6	32.2	5.41	25.5	48.7	6.97	30	6.48	1.32	6.38	1.34	8.42	1.65	5.08	0.762	5.02	0.803	63.5
QH-3	硅质泥岩	2.5	2.4	4.64	112.0	55.8	20.9	2.72	16.5	31	4.41	18.8	3.81	0.802	3.58	0.706	4.26	0.825	2.59	0.405	2.69	0.451	28.2
QH-4	页岩	5.2	3.7	11.3	112.0	62.8	36.8	1.84	32.7	68	9.45	40.3	8.32	1.52	7.11	1.39	8.13	1.51	4.63	0.746	5.16	0.845	47.8
QH-5	页岩	25.0	7.8	11.3	487.0	65.7	67.9	5.46	38.5	66.2	8.97	36.1	6.88	1.41	6.03	1.19	7.33	1.52	4.86	0.804	5.44	0.904	50.6
QH-6	页岩	10.1	6.1	9.02	277.0	57.4	45.0	5.27	31.6	52.4	7.53	31.4	6.47	1.32	6.27	1.29	8.44	1.81	6.01	1.08	7.08	1.19	61
QH-7	页岩	4.3	5.2	7.9	338.0	45.8	29.4	2.94	25.7	39.4	4.64	17	2.91	0.652	2.84	0.615	4.86	1.17	4.26	0.828	5.91	0.974	39
QH-8	页岩	35.7	10.7	7.08	353.0	43.5	63.8	6.05	29.8	51.1	6.95	28.4	5.8	1.22	5.32	1.11	7.32	1.59	5.27	0.922	6.21	1.03	53.2
QH-9	页岩	23.1	8.1	8.26	332.0	50.6	79.9	5.88	31.7	54.3	7.43	30.1	6.11	1.21	5.69	1.12	7.44	1.59	5.45	0.962	6.45	1.06	56.7
QH-10	页岩	43.4	13.4	9.75	348.0	57.8	54.9	4.41	35.8	60.8	8.22	32.5	6.19	1.27	5.74	1.21	7.98	1.73	5.89	1.05	7.03	1.16	57
QH-11	页岩	40.5	11.4	10.1	401.0	54.9	56.6	5.2	32.1	54.6	7.3	29.3	5.4	1.15	5.08	1.06	7.14	1.61	5.43	0.951	6.58	1.08	52.7
QH-12	页岩	19.1	9.8	13.2	454.0	84.1	85.5	10.8	42.6	68.8	7.97	29.4	4.9	1.07	5.11	1.08	7.45	1.73	5.92	1.06	7.28	1.22	59.1
QH-13	页岩	16.2	6.9	12.3	240.0	62.4	46.0	7.42	39.1	68.1	8.78	34.7	6.71	1.39	6.27	1.18	7.01	1.46	4.83	0.809	5.29	0.907	48.1
QH-14	页岩	10.1	6.8	12.8	224.0	60.2	29.5	4.05	37.5	66.4	8.64	34	6.13	1.22	5.68	1.11	6.94	1.5	4.74	0.802	5.14	0.846	47.9
QH-15	页岩	23.1	7.4	12.5	471.0	62.5	77.0	7.38	39.7	68.7	8.71	34.3	6.37	1.3	6.16	1.19	7.36	1.49	5.06	0.884	5.93	0.953	52.9
QH-16	页岩	20.5	7.9	12.6	404.0	62.6	49.9	4.73	36.7	61.3	8.24	32.7	6.5	1.32	5.95	1.21	7.47	1.56	5.17	0.897	5.91	0.945	51.6
QH-17	页岩	26.6	7.9	11	429.0	59.3	50.3	5.97	36.6	66.4	8.73	35.5	6.93	1.34	5.91	1.1	6.83	1.37	4.6	0.756	4.92	0.803	47.2
QH-18	泥岩	21.3	8.6	12.2	431.0	59.3	48.0	6.11	38.8	67.2	8.63	35.1	6.88	1.38	6.22	1.23	7.61	1.58	5.43	0.898	6.06	0.971	53.2
QH-19	泥岩	17.9	6.8	10.4	401.0	59.5	58.8	5.46	33.1	59.4	7.5	29.5	5.46	1.12	4.88	0.933	5.84	1.21	4.02	0.695	4.66	0.753	39.9
QH-20	泥岩	24.7	8.7	12	464.0	66.2	62.6	5.01	37.9	66	8.76	34.6	6.61	1.33	5.88	1.13	7.03	1.45	4.96	0.792	5.42	0.87	48.5
QH-21	泥岩	24.6	8.9	12.9	405.0	65.6	52.4	17.7	39.4	70.5	9.56	39.7	7.66	1.47	7.04	1.31	7.81	1.55	5.24	0.878	5.51	0.87	52.5
QH-22	白云质泥岩	1.6	3.3	11.6	111.0	51.0	17.5	8.87	35.7	66.7	7.99	31.3	5.84	1.13	5.31	0.989	6.21	1.28	4.34	0.72	4.64	0.715	41.1
QH-23	白云质泥岩	1.5	3.5	13.4	116.0	64.5	19.8	8.73	37.2	68.7	8.22	33.3	6.74	1.34	6.04	1.14	6.77	1.37	4.59	0.731	4.97	0.803	44
QH-24	白云质泥岩	0.9	3.0	12.8	101.0	57.5	15.6	9.93	38	71.6	8.41	33.8	6.33	1.22	5.63	1.06	6.27	1.28	4.38	0.727	4.64	0.776	40.7
QH-25	白云质泥岩	0.7	3.1	13.9	101.0	59.7	18.1	6.98	37.9	71.1	8.92	37.4	8.08	1.65	7.14	1.34	7.9	1.58	5.12	0.87	5.69	0.914	52.2
QH-26	白云质泥岩	0.5	2.9	13.3	78.0	55.6	19.3	11.2	39.7	73.7	9.2	37.9	7.56	1.4	6.55	1.18	7.02	1.42	4.72	0.769	5.4	0.859	45.4
QH-27	白云质泥岩	0.4	2.1	10.3	43.0	35.1	12.2	5.67	28.7	53.9	6.61	26.7	5.28	1	4.99	0.972	5.96	1.21	4.02	0.685	4.5	0.704	38.9
QH-28	白云质泥岩	0.4	2.5	12.1	62.0	51.2	16.2	6.52	34.7	66	8.36	34.9	6.54	1.2	6.05	1.13	6.62	1.35	4.53	0.75	5.25	0.851	41.2
QH-29	白云质泥岩	0.3	1.8	9.63	47.0	35.4	12.9	5.89	26.8	47.4	5.64	22.4	4.43	0.86	4.21	0.842	5.38	1.11	3.64	0.603	4.21	0.647	35.6

平均14.2×10⁻⁶；Th为4.64×10⁻⁶~13.9×10⁻⁶，平均10.7×10⁻⁶；Co为1.12×10⁻⁶~17.71×10⁻⁶，平均6.37×10⁻⁶；U为1.84×10⁻⁶~13.4×10⁻⁶，平均6.17×10⁻⁶。

稀土元素：检测出La、Ce、Dy、Eu、Y、Ho等15种稀有元素(表2，图4b)。从图中可以看出，测试样品明显具有轻稀土富集、重稀土亏损的特点。其中稀土元素总量(ΣREE)为90.82×10⁻⁶~198.49×10⁻⁶，平均值为167.60×10⁻⁶，高于全球平均大陆地壳成分146.4×10⁻⁶(Taylor and Mclennan.，1985)，低于澳大利亚新太古界页岩的平均值(173.2×10⁻⁶)(Pourmand et al.，2012)。轻稀土元素总量(ΣLREE)为75.32×10⁻⁶~169.46×10⁻⁶，平均值为140.85×10⁻⁶，占总量的84.04%。重稀土元素(ΣHREE)为14.69×10⁻⁶~33.17×10⁻⁶，平均值为26.75×10⁻⁶，占总量的15.96%。

5 讨 论

5.1 沉积物来源

沉积岩中的化学组分一般有3个主要来源：陆源碎屑物质、生物作用来源以及自生海水来源(Piper，1994)。由于元古宙海洋与显生宙、现代海洋环境水体化学环境有所差异，且太古宙以后各时代随时代的变新沉积岩中的稀土含量增加，但分布模式不变(Nance and Taylor，1976；于炳松和裴愉卓，1998)。研究表明，稀土元素和海水滞留时间比较短的不相容元素可有效应用于元古界沉积物源分析(解启来等，2003；蓝廷广等，2012；王浩等，2012；杨世文等，2016)。

沉积物的粒度对Th的影响比较小，可将Th作
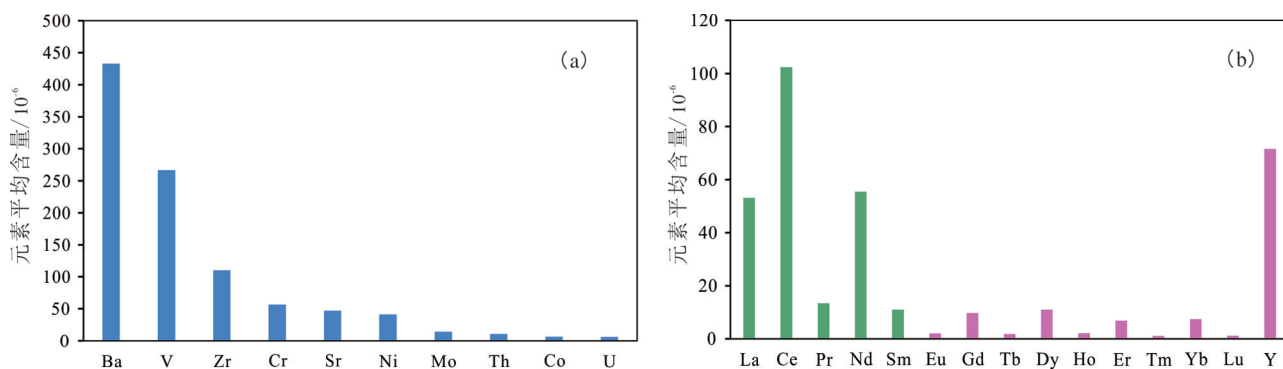
图4 微量元素和稀土元素平均含量直方图
Fig.4 Histogram of average content of trace elements and rare earth elements

为指标来衡量陆源碎屑组分(Johnson and Grimm, 2001)。研究表明,黑色页岩的成岩过程对Zr、Y/Ho的影响比较小,因此利用Th-Zr和Th-Y/Ho可以有效地指示陆源碎屑对成岩的贡献(Schroder and Grotzinger, 2007)。洪水庄组样品中Th-Zr和Th-Y/Ho的关系图(图5)显示两者不存在明显的相关关系,说明黑色页岩中元素的来源并不单一为陆源碎屑物质,部分元素为海水自生来源。

海洋垂直分布Y/Ho比值也可以用来判别沉积物是来自于陆源碎屑还是海水沉积(Zhang et al., 1994)。Y和Ho具有相似的离子半径,并具有相似的物理化学性质(Zhang et al., 1994)。由于沉积物在水柱中对Ho的捕捉能力大约是Y的2倍(Bau, 1996a; Zhang and Nozaki, 1996; Nozaki et al, 1997),以陆源碎屑为主要来源的沉积物具有均匀且较低的Y/Ho比值,一般介于26~28(Balz and Gregory, 2001),上地壳和页岩的Y/Ho平均值介于25~30(Mclennan, 2013),海水沉积物的Y/Ho比较高,变化区间大,但一般都介于60~70(Balz and Gregory, 2001)。洪水庄组样品中的Y/Ho为30.5~38.5,平均值为33.2,介于球粒陨石和海水之间,说明洪水庄组沉积物不仅有海水沉积成分,也有陆源碎屑的成分(Bau and Dulski, 1996b)。研究表明,随着海水沉积物的稀土元素逐步被陆源碎屑沉积物的稀土元素混入和叠加,Y/Ho比值有随着ΣREE含量增大有减小的趋势(Chen et al, 2015; Zhang et al, 2016)。从海水(Y/Ho=60)和UCC陆源碎屑(Y/Ho=27.5)的混合沉积百分比趋势中(图6)可以看出,洪水庄组样品沉积物来源中海水沉积所占比例介于10%~20%。

沉积岩中,稀土元素含量及分布模式与沉积物来源和沉积环境有着密切联系(Wilde et al., 1996; Bellanca et al., 1997)。Eu^{2+}一般出现在与岩浆活动有关的下地壳强高温还原环境中(Michard, 1989; German et al., 1999),火山热液物质会造成沉积物出现Eu正异常特征(Chen et al., 2006)。正常的海水具有轻稀土富集和Ce负异常特征。洪水庄组沉积物稀土元素经过澳大利亚页岩(PAAS)标准化后(Pourmand et al., 2012),呈现轻稀土元素相对亏损、重稀土相对富集的左倾型配分模式(图7)。Ce异常值为0.82~0.97,平均值为0.89,为负异常。且Eu异常值为1.01~1.20,平均值为1.11,普遍呈正异常(表2)。

由于洪水庄组沉积期,主要以被动大陆边缘构造–沉积环境为特征,构造环境相对稳定,浅海沉积体系总体成面状分布,所以形成以滨岸和陆棚环境为主的碳酸盐岩和细碎屑岩混积体系(曲永强等, 2010)。野外露头也发现有硅质页岩的存在(图2a),而硅质岩的地球化学特征表明热水成因硅质岩与火山岩共生、非热水成因硅质岩与沉积岩共生且均形成于被动大陆边缘的海相、海陆交互相等环境(徐勇航等, 2008;李红中等, 2012)。此外,华北克拉通北部在中元古代地幔发生一系列强烈隆升,其盆山构造属于典型地幔亚热柱,同时伴随有广泛分布的元古宙火山岩侵入体(Zhai et al 2000; Menzies et al., 2007; 乔秀夫等, 2007)。因此,结合其沉积构造背景分析,认为洪水庄组不仅具有陆源碎屑和海水沉积混积特征,还可能有火山碎屑成分。

5.2 氧化还原条件

氧化还原敏感元素指那些溶解度明显受沉积环境氧化还原控制而导致其向还原性水体和沉积物中迁移而自生富集的微量元素,主要包括Mo、V、

表2 华北北部中元古界清河剖面洪水庄组样品微量元素数据相关计算结果

Table 2 Calculation results of trace element data of Hongshuizhuang Formation from Qinghe section of Middle Proterozoic in northern part of North China

样品编号	SiO$_2$/Al$_2$O$_3$	K$_2$O/Na$_2$O	K$_2$O/(Na$_2$O+CaO)	TFe$_2$O$_3$+MgO	V/Cr	δU	U-ef	Mo-ef	Y/Ho	REE/10^{-6}	LREE/10^{-6}	HREE/10^{-6}	(Nd/Yb)$_N$	Eu/Eu*	Ce/Ce*
QH-1	13.64	35.51	3.60	0.95	2.69	1.13	2.77	5.60	33.74	111.43	96.74	14.69	0.91	1.05	0.96
QH-2	9.91	33.88	3.95	1.09	5.12	1.44	4.53	22.31	40.02	148.43	118.97	29.46	0.48	1.09	0.88
QH-3	16.53	29.89	3.59	1.03	2.01	1.22	2.81	9.11	35.55	90.83	75.32	15.51	0.56	1.15	0.87
QH-4	6.58	41.06	3.82	1.17	1.78	0.99	2.06	8.88	32.92	189.81	160.29	29.52	0.63	1.05	0.93
QH-5	5.15	44.86	8.83	1.97	7.41	1.35	3.65	36.43	34.62	186.14	158.06	28.08	0.54	1.16	0.86
QH-6	6.33	38.07	10.18	1.43	4.83	1.34	3.31	17.00	35.05	163.89	130.72	33.17	0.36	1.10	0.82
QH-7	7.64	38.80	11.11	1.25	7.38	1.33	3.16	8.08	34.67	111.76	90.30	21.46	0.23	1.20	0.86
QH-8	8.34	29.14	6.74	2.01	8.11	1.64	7.55	78.09	34.80	152.04	123.27	28.77	0.37	1.17	0.86
QH-9	7.36	34.55	5.95	1.85	6.56	1.49	5.06	45.06	37.09	160.61	130.85	29.76	0.38	1.09	0.85
QH-10	6.15	37.64	9.94	1.98	6.02	1.61	7.43	74.64	34.27	176.57	144.78	31.79	0.37	1.13	0.85
QH-11	5.78	39.72	10.84	2.18	7.30	1.54	6.06	99.03	34.04	158.78	129.85	28.93	0.36	1.16	0.86
QH-12	5.10	44.40	15.27	1.75	5.40	1.38	4.41	26.80	35.53	185.59	154.74	30.85	0.33	1.13	0.90
QH-13	4.74	47.28	12.68	1.94	3.85	1.25	3.01	21.98	34.26	186.54	158.78	27.76	0.53	1.14	0.89
QH-14	4.60	50.55	24.35	1.65	3.72	1.23	2.82	13.10	33.21	180.65	153.89	26.76	0.53	1.10	0.89
QH-15	4.98	45.92	13.89	2.10	7.54	1.28	3.38	32.83	36.92	188.11	159.08	29.03	0.47	1.10	0.89
QH-16	4.70	49.44	12.76	1.89	6.45	1.31	3.47	27.77	34.40	175.87	146.76	29.11	0.45	1.13	0.85
QH-17	5.07	45.47	11.68	2.07	7.23	1.36	3.67	38.38	35.83	181.79	155.50	26.29	0.58	1.11	0.89
QH-18	4.70	46.91	11.97	1.86	7.27	1.36	3.78	28.90	35.02	187.99	157.99	30.00	0.47	1.12	0.88
QH-19	5.75	46.40	14.31	2.06	6.74	1.33	3.47	28.22	34.29	159.07	136.08	22.99	0.51	1.15	0.91
QH-20	5.01	45.43	11.06	1.95	7.01	1.37	3.98	35.07	34.79	182.73	155.20	27.53	0.52	1.13	0.87
QH-21	4.34	43.18	10.00	2.55	6.17	1.35	3.79	32.42	35.23	198.50	168.29	30.21	0.58	1.06	0.87
QH-22	4.55	48.79	1.01	6.45	2.18	0.92	1.68	2.48	33.39	172.86	148.66	24.20	0.54	1.08	0.95
QH-23	4.59	50.42	3.74	3.86	1.80	0.88	1.54	2.10	33.40	181.91	155.50	26.41	0.54	1.11	0.95
QH-24	4.45	52.58	2.19	4.79	1.76	0.82	1.34	1.21	33.07	184.12	159.36	24.76	0.59	1.08	0.97
QH-25	4.67	51.72	14.15	2.94	1.69	0.80	1.29	0.87	34.36	195.60	165.05	30.55	0.53	1.15	0.93
QH-26	4.50	54.63	6.16	3.68	1.40	0.79	1.22	0.66	33.25	197.38	169.46	27.92	0.57	1.06	0.93
QH-27	4.87	43.27	0.46	9.25	1.33	0.76	1.35	0.72	33.43	145.23	122.19	23.04	0.48	1.03	0.94
QH-28	4.71	41.79	1.04	7.14	1.20	0.77	1.29	0.70	31.74	178.23	151.70	26.53	0.54	1.01	0.93
QH-29	4.57	39.73	0.42	10.16	1.33	0.73	1.16	0.62	33.35	128.172	107.53	20.642	0.43	1.06	0.93

注：标准化数据采用文献Pourmand et al., 2012；Eu/Eu* = 2Eu$_N$/(Sm$_N$+Gd$_N$)。

Ni、Co、Cr，U 等（Francois, 1988；Russell and Morford, 2001）。由于微量元素会受到陆源组分的影响，简单的利用微量元素绝对含量来判断水体的氧化还原条件并不准确(白忠凯等，2018)。利用V/Cr、Ni/Co指标可以示踪和恢复古环境氧化还原状态（Hatch and Leventhal, 1992; Jones and Manning, 1994；陈孝红等，2018）。V/Cr > 4.25 为厌氧环境，2.00~4.25 为贫氧环境，< 2.00 为富氧环境。Ni/Co > 7 为厌氧环境，介于 5 ~ 7 为贫氧环境，< 5 为富氧环境。δU=[2U/(U+Th/3)] > 1 为厌氧环境，< 1 为富氧环境（吴朝东和陈其英，1999）。Mo 含量在 5×

10^{-6}~40×10^{-6}以上可指示沉积物形成于静海还原条件(Piper, 1994; Crusius et al., 1996)。虽然不同学者对于这些元素及比值所反映的沉积环境划分方法有所差异，但基本上都认为沉积环境还原程度增强，这些参数值也相应增加。

根据判别标准，利用 Ni/Co、V/Cr、δU 和 Mo 关系图对洪一段和洪二段的氧化还原环境进行恢复，结果（图8）显示出良好的一致性：洪一段泥页岩类形成于贫氧和厌氧环境，洪二段白云岩类形成于正常的氧化环境。这种不同的氧化还原状态可能是由于水体的深度变化引起的，一般在深水条件下更
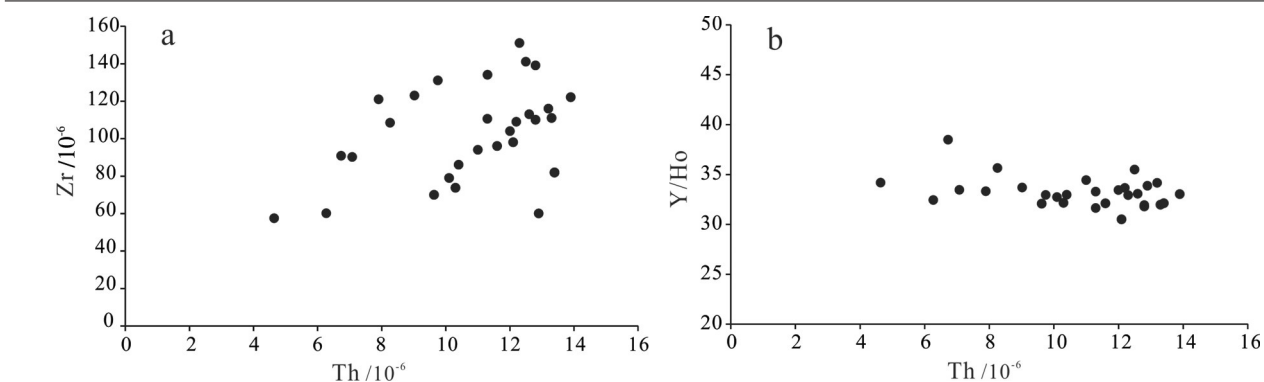
图5 洪水庄组样品Th−Zr(a),Th−YHo(b)关系图解
Fig.5 Th−Zr, Th−Y/Ho relationship diagram of samples from Hongshuihzhuang Formation rocks

容易成缺氧环境(Zhou et al., 2015)。

　　近年来,Algeo and Tribovillard(2009)首次提出利用沉积物U/Mo比值及其富集系数(用Mo−EF和U−EF表示)来限定沉积盆地内颗粒传输机制和过程。通过对现代海洋的研究,建立了非滞留、弱滞留和强滞留3种海洋环境下的U−Mo协变模式(Tribovillard et al., 2012)。U−Mo协变模式能同时识别海盆水体滞留情况和氧化还原条件。以东太平洋为代表的非滞留环境为例,在贫氧条件下,由于U富集开始于Fe(Ⅲ)−Fe(Ⅱ)氧化还原反应界限,早于Mo的富集,使Mo/U比值为正常海水的0.1~0.3倍。随着水体还原程度的增强,Mo在沉积物中的富集速率超过U,使沉积物中的Mo/U比值增大,为正常海水的1~3倍;在Caricao Basin为代表的弱滞留环境中,由于金属氢氧化物颗粒作为载体能加强水中的Mo进入沉积物中的速率,Mo/U比值通常是海水的3~10倍;以黑海为代表的强滞留环境中,Mo/U比值很低,一般小于正常海水值,且Mo/U比值在厌氧环境中会随着富集系数的增加而降低,这是由于强烈的盆地滞留限制了U和Mo的重新补给,而沉积物对Mo的吸收速率大于U,导致海水中的Mo比U更加亏损。

　　现代海洋环境硫化海域所占的面积仅0.3%或不到,元古宙硫化海域所占的面积较大,相当于现代全球海洋面积的30%~40%。这种条件下Mo总
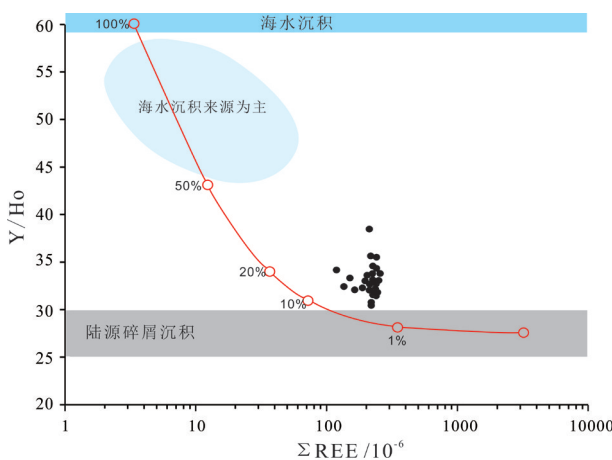
图6 洪水庄组样品物源百分含量识别图(底图据Zhang et al, 2016)
注:红色曲线代表的是海水沉积和UCC陆源碎屑沉积混合含量的百分比趋势;百分数代表的是海水沉积百分比
Fig.6 Percentage identification chart of source material in Hongshuizhuang Formation(after Zhang et al., 2016)
(The red curve represents the percentage trend of the mixing content of seawater deposition and UCC terrigenous clastic deposition. The percentage represents the percentage of seawater sediments)
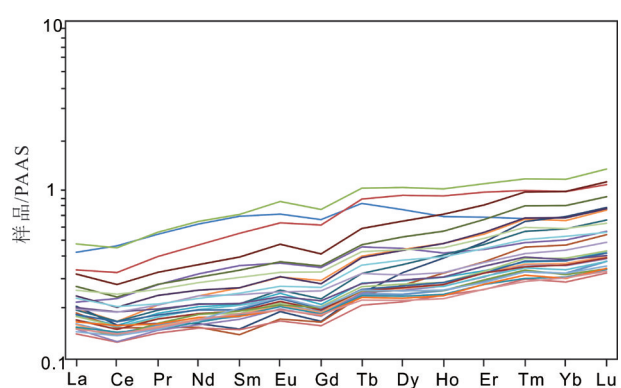

图7 澳大利亚页岩标准化(PAAS)后洪水庄组泥页岩样品稀土元素分布模式(数据来源于Pourmand et al., 2012)
Fig.7 REE distribution pattern of Hongshuizhuang formation shale samples after shale standardization in Australia(data from Pourmand et al., 2012)
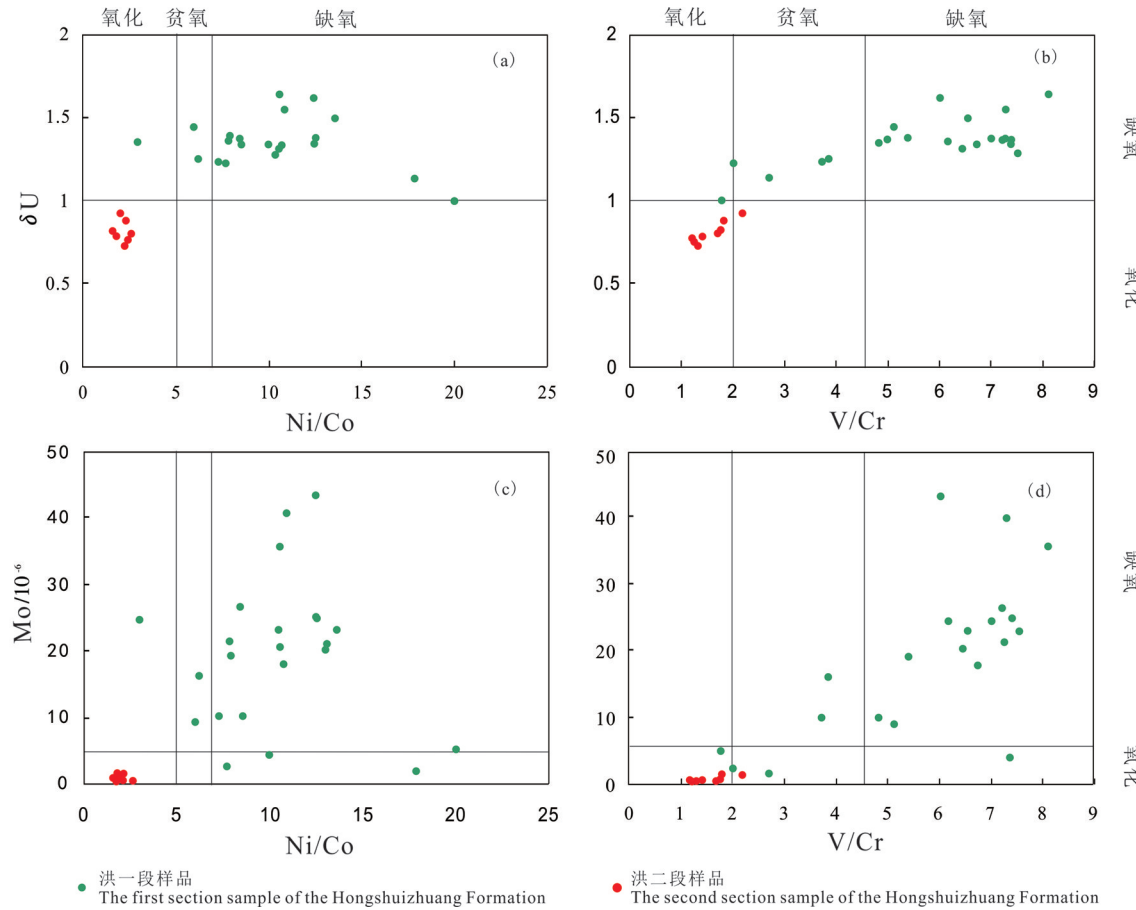
图8 洪水庄组样品氧化还原参数交会图
a—δU−Ni/Co图; b—δU −V/Cr图; c—Mo− Ni/Co图; d—Mo− V/Cr图
Fig.8　Rendezvous of redox parameters of the Hongshuizhuang Formation samples
a−δU−Ni/CO diagram; b−δU−V/Cr diagram; c−Mo−Ni/CO diagram; d−Mo−V/Cr diagram

量会在硫化水体中过量沉降,造成元古宙海洋的
Mo浓度远远低于现代海洋水平(Lyons et al.,
2009)。且由于元古宙海洋环境富铁(Canfield,
1998),沉积物能够吸收更多的U元素,而Mo的吸
收量不变,导致中元古代海洋和沉积物中Mo/U比
值均比现代海洋和沉积物低,约为现代海洋和沉积
物1/3(Algeo and Tribovillard, 2009)。由于中元古
代海洋和沉积物Mo/U比值是同步偏低,借鉴于U−
Mo协变模式,可用于分析洪水庄组古海盆的氧化
还原和水体滞留情况。

　　从图9中可以看出,在洪一段沉积期,水体还原
程度的增强,Mo−EF和U−EF值较高,水体还原程度
强,处于厌氧−硫化环境。Mo元素富集较U快,造成
Mo−EF/U−EF比值接近于正常海水的1~3倍;在洪
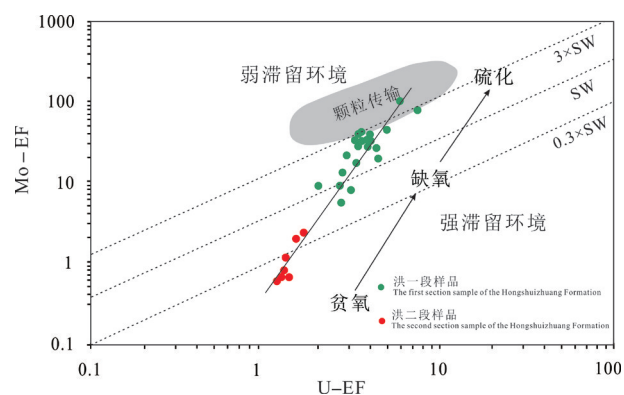
图9 洪水庄组样品Mo−EF和U−EF协变图
Mo−EF=(U/Al) sample / (U/Al)$_{PAAS}$),U−EF=(Mo/Al) sample/
(Mo /Al)$_{PAAS}$
Fig.9　Mo−EF and U−EF covariant diagram of
Hongshuizhuang Formation samples

二段沉积期，Mo和U富集系数低，水体还原性差，为贫氧环境。Mo-EF/U-EF 比值也低，为正常海水的0.3倍，分布在贫氧-厌氧区域，这些变化特征与海洋非滞留海盆环境基本一致。不同的是，中元古代Mo-EF/U-EF 相比于现代海洋的"强滞留环境"和"弱滞留环境"的Mo-EF/U-EF 有向左偏移现象（即较低的U-EF值可对应任何特定的Mo-EF值）。

综上分析表明，洪水庄组沉积环境为非滞留海盆，氧化还原条件在沉积过程中发生了演变，且早期为厌氧-硫化环境，晚期还原程度降低，演变为贫氧-厌氧环境。这种演变与垂直升降构造背景以及沉积海平面变化密切相关，雾迷山组、洪水庄组和铁岭组作为一个大的沉积旋回，其二级海平面发生过多次海侵和海退，为滨海和陆棚沉积环境（梅冥相等，1998；曲永强等，2010）。受铁岭上升、芹峪上升等区域构造运动的影响，洪水庄组沉积早期海平面上升，晚期至铁岭组沉积期海平面发生下降（旷红伟等，2009），导致其氧化还原条件也发生了变化。

6　结　论

（1）洪水庄组沉积物来源具有混积特征，不仅有陆源碎屑物质，还有海水沉积物。其中海水沉积物来源占比介于10%~20%。此外，稀土元素分布模式以及Ce和Eu异常暗示沉积物来源有火山热液活动的参与。

（2）Mo-EF/U-EF 分析结果表明洪水庄为海洋非滞留海盆沉积环境，氧化还原条件在沉积期发生了演变：在洪一段沉积时期，水体还原程度强，为厌氧-硫化环境；洪二段沉积时期，水体还原程度降低，为贫氧-厌氧环境。这种沉积环境的演变与构造背景以及海平面变化密切相关。

References

Algeo T J, Tribovillard N. 2009. Environmental analysis of paleoceanographic systems based on molybdenum- uranium covariation[J]. Chemical Geology, 268: 211-225.

Bai Zhongkai, Xie Li, Han Miao, LV Xiuxiang, Sun Zhichao, Li Qinyao, Yang Youxing, Zhang Jinhu. 2018. Paleoproductivity conditions of lower member of Cambrian Xiaoerbulak Formation in Kalpin thrust belt, Tarim Basin[J]. Geology in China, 45(2): 227-236(in Chinese with English abstract).

Balz S K, Gregory E W. 2001. The geochemistry of Late Archaean microbial carbonate: Implications for ocean chemistry and continental erosion history[J]. Geochimica et Cosmochimica Acta, 65(15): 2509-2525.

Bau M. 1996a. Controls on the fractionation of isovalent trace elements in magmatic and aqueous systems: Evidence from Y/Ho, Zr/Hf, and lanthanide tetrad effect[J]. Contributions to Mineralogy & Petrology, 123(3):323-333.

Bau M, Dulski P. 1996b. Distribution of yttrium and rare earth elements in the Penge and Kuruman iron- formations, Transvaal Supergroup, South Africa[J]. Precambrian Research, 79, 37-55.

Bellanca A, Masetti D, Neri R. 1997. Rare earth elements in limestone/ marlstone couplets from the Albian- Cenomanian Cismon section (Venetian region, northern Italy): Assessing REE sensitivity to environmental changes[J]. Chemical Geology, 141(3/4):141-152.

Canfield D E. 1998. A new model for Proterozoic ocean chemistry[J]. Nature,396 (6710): 450-453.

Chang Huajin, Chu Xuelei, Feng Lianjun, Huang Jing, Zhang Qirui. 2009. Redox sensitive trace elements as Paleoenvironments Proxies[J]. Geological Review, 55(1):91- 99(in Chinese with English abstract).

Chen Jianfa, Sun Shengli 2004. Preliminary study of geochemical characteristics and formation of organic matter rich stratigraphy of Xiamaling Formation of Late Proterozoic in North China[J]. Natural Gas Geoscience, 15(2): 110-114(in Chinese with English abstract).

Chen Daizhao, Qing Hairuo, Yan Xin, Li He. 2006. Hydrothermal venting and basin evolution (Devonian, South China): Constraints from rare earth element geochemistry of chert[J]. Sediment Geology, 183: 203-216.

Chen J, Algeo T J, Zhao L, Chen Z Q, Cao L, Zhang L, Li Y. 2015. Diagenetic uptake of rare earth elements by bioapatite, with an example from Lower Triassic conodonts of South China[J]. Earth-Science Reviews, 149(3):181-202.

Chen Xiaohong, Wei Kai, Zhang Baomin, Li Peijun, Li Hai, Liu An, Luo Shengyuan. 2018. Main geological factors ontrolling shale gas reservoir in the Cambrian Shuijingtuo Formation in Yichang of Hubei Province as well as its and enrichment patterns[J]. Geology in China, 45(2): 207-226(in Chinese with English abstract).

Crusius J, Calvert S E, Pedersen T F, Sage D. 1996. Rhenium and molybdenum enrichments in sediments as indicators of oxic, suboxic, and sulfidic conditions of deposition[J]. Earth Planet Science Letter, 145: 65-78

Fang Jie, Liu Baoquan, Jin Fengming, Liu Jinqiang, Yu Zhanwen. 2002. Source potential for generating hydrocarbon and exploration prospects of Middle- Upper Proterozoic in the Northern China[J]. Acta Petrolei Sinica, 23(4): 18- 24(in Chinese with English abstract).

Francois R. 1988. A study on the regulation of the concentrations of some trace metals (Rb, Sr, Zn, Pb, Cu, V, Cr, Ni, Mn and Mo) in Saanich Inlet sediments, British Columbia, Canada[J]. Mar. Geology, 83: 285-308.

German C R, Hergt J, Palmer M R, Edmond J M. 1999. Geochemistry of a hydrothermal sediment core from the OBS vent−field, 21°N East Pacific Rise[J]. Chemical Geology, 155: 65−75.

Hao Shisheng. 1990. Neoproterozoic− Mesoproterozoic Petroleum Geology in north China[M]. Dongying: Petroleum University Press.

Hatch J R, Leventhal J S. 1992. Relationship between inferred redox potential of the depositional environment and geochemistry of the Upper Pennsylvanian (Missourian) stark shale member of the Dennis limestone, Wabaunsee County Kansas,U.S.A[J]. Chemical Geology, 9(1/3): 65−82.

Huo Yong, Luo Shunshe, Zhang Jiankun, Pang Qiuwei, Jin Shanshan, Shang Fei. 2012. Sedimentary Facies and sequence stratigraphic framework of Hongshuizhuang− Tieling Formation in Xuanlong Depression of Yanshan Region[J]. Geological Science and Technology Information, 31(3): 11− 18(in Chinese with English abstract).

Lai X Q, Fu C D, Liang Q I, Pei C X. 2003. Ree geochemistry of doushantuo phosphorites and paleoenvironmental changes in Weng'an area, South China[J]. Acta Mineralogica Sinica, 23(4): 289−295.

Luo Shunshe, Lü Qiqi, Li Linjing, Dan Weidong. 2012. Depositional environment of Hongshuizhuang and Tieling Formation in the Xuanlong Depression, Yanshan region[J]. Marine Geology Frontiers,(2):10−16(in Chinese with English abstract).

Luo Qingyong, Zhong Ningning, Zhu Lei, Yan Nian, Qin Jing, Qi Lin, Zhang Yi, Ma Yong. 2013. Correlation of burial organic carbon and paleoproductivity in the Mesoproterozoic Hongshuizhuang Formation, northern North China[J]. Chin. Sci. Bull., (11):1036−1047(in Chinese).

Li Chao, Peng Pingan, Sheng Guoying, Fu Jiamo, Yan Yuzhou. 2003. A molecular and isotopic geochemical study of Meso− Neoproterozoic(1.73−0.85 Ga) sediments from the Jixian section, Yanshan Basin, North China[J]. Precambrian Research, 125: 337−356.

Li Hongzhong, Zhou Yongzhang, Zhang Lianchang, He Junguo, Yang Zhijun, Liang Jin, Zhou Liuyu, Wa Xi Lali. 2012. Study on geochemistry and development mechanism of Proterozoic chert from Xiong'er Group in southern region of North China Craton[J]. Acta Petrologica Sinica, 28(11) : 3679− 3691(in Chinese with English abstract).

Lyons T W, Anbar A D, Severmann S, Scott C, Gill B C. 2009. Tracking euxinia in the ancient ocean: A multiproxy perspective and Proterozoic case study[J]. Annual Review of Earth and Planetary Sciences, 37(1):507−534.

Jones B, Manning D A. 1994. Comparison of geochemical indices used for the interpretation of palaeoredox conditions in ancient mudstones[J].Chemical Geology, 111(111): 111−129.

Johnson K M, Grimm K A. 2001. Opal and organic carbon in laminated diatomaceous sediments: Saanich Inlet, Santa Barbara Basin and the Miocene Monterey Formation[J]. Marine Geology, 174(1):159−175.

Kuang Hongwei, Li Jiahua, Peng Nan, Luo Shunshe, Cen Chao. 2009. The C and O isotopic compositions and their evolution recorded in the carbonate interval of the Yanshan area from 1.6 to 1.0 Ga, and their geological implications[J]. Earth Science Frontiers, 16(5): 118−133(in Chinese with English abstract).

Lan Tingguang, Fan Hongrui, Hu Fangfang,Yang Kuifeng, Zheng Xiaoli, Zhang Huadong. 2012. Geological and geochemical characteristics of Paleoproterozoic Changyi banded iron formation deposit，Jiaodong Peninsula of eastern China[J]. Acta Petrologica Sinica, 28(11): 3595−3611(in Chinese with English abstract).

Li Huaikun, Zhu Shixing, Xiang Zhenqun, Su Wenbo, Lu Songnian, Zhou Hongying, Geng Jianzhen, LI Sheng, Yang Fengjie, Li Huaikun. 2010. Zircon U− Pb dating on tuff bed from Gaoyuzhuang Formationin Yanqing, Beijing, and further constraints on the new subdivision of the Mesoproterozoic stratigraphy in the northern North China Craton[J]. Acta Petrologica Sinica, 26(7): 2131 − 2140(in Chinese with English abstract).

Mclennan S M. 2013. Relationships between the trace element composition of sedimentary rocks and upper continental crust[J]. Geochemistry Geophysics Geosystems, 2(4):1021−1024.

Menziesa Martin, Xu Yigang, Zhang Hongfu, Fan Weiming. 2007. Integration of geology, geophysics and geochemistry: A key to understanding the North China Craton[J]. Lithos, 96(1):1−21.

Michard A. 1989. Rare earth element systematics in hydrothermal fluids[J]. Geochimica et Cosmochimica Acta, 53: 745−750.

Mei Mingxiang, Li Zhizhong, Bai Zhida, Xu Debin. 1998. Preliminary study on the Middle and Upper Proterozoic cyclic−sequences in Xinlong County, Hebei[J]. Journal of Stratigraphy, 22(2): 102−10.

Nance W B, Taylor S R. 1976. Rare earth element patterns and crustal evolution− I. Australian post− Archean sedimentary rocks[J]. Geochimica et Cosmochimica Acta, 40(12):1539−1551.

Nozaki Y, Zhang J, Amakawa H. 1997. The fractionation between Y and Ho in the marine environment[J]. Earth and Planetary Science Letters, 148: 329−340.

Piper D Z. 1994. Seawater as the source of minor elements in black shales, phosphorites, and other sedimentary deposits[J]. Chemical Geology, 115: 95−114.

Pourmand A, Dauphas N, Ireland T J. 2012. A novel extraction chromatography and MC−ICP−MS technique for rapid analysis of REE, Sc and Y：Revising CI− chondrite and Post− Archean Australian Shale (PAAS) abundances[J]. Chemical Geology, 291: 38−54.

Qiao Xiufu,Gao Linzhi, Zhang Chuanheng. 2007. New idea of the Meso− Neoproterozoic chronostratigraphic chart and tectonic environment in Sino− Korean plate[J]. Geological Bulletin of China, 26(5): 503−509(in Chinese with English abstract).

Qin Jing, Zhong Ningning, Qi Wen, Zhang Yanqi, Luo Qingyong. 2010. Organic Petrology of the Hongshuizhuang Formation in northern of North China[J]. Oil & Gas Geology, 31(3): 367−374(in Chinese with English abstract).

Qu Yongjiang, Meng Qianglin, Ma Shouxian, Li Lin, Wu Guoli. 2010. Geological characteristics of unconformities in Mesoproterozoic successions in the northern margin of North China Block and their tectonic implications[J]. Earth Science Frontiers, 17(4):112−127(in Chinese with English abstract).

Russell A D, Morford J L. 2001. The behavior of redox sensitive metals across a laminated massive−laminated transition in Saanich Inlet, British Columbia[J]. Marine Geology, 174(1/4): 341−354.

Schroder S, Grotzinger J P. 2007. Evidence for anoxia at the Ediacaran−Cambrian boundary: The record of redox−sensitive trace elements and rare earth elements in Oman[J]. Journal of the Geological Society, 164(1):175−187.

Sun Xingli, Chen Jianfa, Liu Wenhui, Zhang Shuichang, Wang Darui. 2003. hydrothermal venting on the seafloor and formation of organic−rich sediments−evidence from the Neoproterozoic Xiamaling Formation, North China[J]. Geological Review, 49(6): 588−595(in Chinese with English abstract).

Taylor S R, Mclennan S M. 1985. The Continental Crust: Its Composition and Evolution, An Examination of the Geochemical Record Preserved in Sedimentary Rocks[M]. Beijing: Science Press.

Tribovillard N, Algeo T J, Baudin F, Riboulleau A. 2012. Analysis of marine environmental condition based on molybdenum−uranium covariation−applications to Mesozoic paleoceanography[J]. Chemical Geology, 324/325: 46−58.

Wang Hao, Ling Wenli, Duan Ruichun, Yang Hongmei, Chen Ziwan, Qin Yadong. 2012. Os isotopic geochemistry of Neoproterozoic−Cambrian black shales in Eastern three gorges of Yangtze Craton and its geological significance[J]. Earth Science, 37(3):451−462.

Wang Tieguan, Han Keyou. 2011. On Meso−Neoproterozoic primary petroleum resources[J]. Acta Petrolei Sinica, 1(1): 1−7(in Chinese with English abstract).

Wang Jie, Chen Jianfa. 2001. The study of depositional environment and hydrocarbon potential of source rocks of Neo−Mesoproterozoic in North China[J]. Natural Gas Geoscience, 12(3): 27−33(in Chinese with English abstract).

Wilde P, Quinby−Hunt M S, Erdtmann B D. 1996. The whole−rock cerium anomaly:A potential indicator of eustatic sea−level changes in shales of the anoxic facies[J]. Sedimentary Geology, 101(1/2): 43−53.

Wu Chaodong, Yang Chenyun, Chen Qiying. 1999. The origin and geochemical characteristics of Upper Sinain−Lower Cambrian black shales in Western Hunan[J]. Acta Petrologica et Mineralogica, 18(1): 26−39(in Chinese with English abstract).

Wu Yinye Y, Liu Wei, Liu Yab, Fang Xiang, Ma Kui. 2016. The underlying deposition of Cambrian of Gondwana in China and its petroleum geological significance[J]. Acta Petrolei Sinica, 37(9): 1069−1079 (in Chinese with English abstract).

Xu Yonghang, Zhao Taiping, Hu Junliang, Chen Wei. 2008. Geochemical characteristics and sedimentary environments of cherts from the Paleoproterozoic Xiong'er Group in the southern part of the North China Block[J]. Acta Sedimentologica Sinica, 56(6): 355−356 (in Chinese with English abstract).

Yang Shiwen, Lou Fasheng, Yang Kunguang, Zhang Fangrong, Ling Guoqing, Cao Yuanbing. 2016. The geochemical characteristics and tectonic significance of metasedimentary rocks in Sinian−Cambrian Xunwu rock group, southern Jiangxi Province[J]. Geology in China, 43(1): 349−364 (in Chinese with English abstract).

Yu Bingsong, Qiu Yuzhuo. REE characteristics in Neoproterozoic to Triassic sedimentary rocks and its relation to crustal evolution in Guizhou Province [J]. Geoscience, 12(2):173−179.

Zhang Lei, Algeo T J, Cao Ling, Zhao Laishi, Chen Zhongqiang, Li Zhihong. 2016. Diagenetic uptake of rare earth elements by conodont apatite[J]. Palaeogeography Palaeoclimatology Palaeoecology, 458, 176−197.

Zhang J, Amakawa H, Nozaki Y. 1994. The comparative behaviors of yttrium and lanthanides in the seawater of the North Pacific[J]. Geophysical Research Letters, 21(24):2677−2680.

Zhang Jing, Nozaki Y. 1996. Rare earth elements and yttrium in seawater: ICP−MS determinations in the East Caroline, Coral Sea, and South Fiji basins of the western South Pacific Ocean[J]. Geochimica et Cosmochimica Acta, 60(23): 4631−4644.

Zhao Wenzhi, Hu Suyun, Wang Zecheng, Zhang Shuichang, Wang Tongshan. 2018. Petroleum geological conditions and exploration importance of Proterozoic to Cambrian in China[J]. Petroleum Exploration and Development, 45(1): 1−13 (in Chinese with English abstract).

Zhou Lian, Algeo T J, Shen Jun, Hu Zhifang, Gong Hongmei, Xie Shucheng, Huang Junhua, Gao Shan. 2015. Changes in marine productivity and redox conditions during the Late Ordovician Hirnantian glaciations[J]. Palaeogeography, Palaeoclimatology Palaeoecology, 420: 223−234.

Zhai Minguo, Bian Aiguo, Zhao Taiping. 2000. The amalgamation of the supercontinent of North China Craton at the end of Neo−Archaean and its breakup during late Palaeoproterozoic and Meso−Proterozoic[J]. Science in China(Series D): Earth Sciences, 43(1): 219−232.

附中文参考文献

白忠凯, 谢李, 韩淼, 吕修祥, 孙智超, 李清瑶, 杨有星, 张金虎. 2018. 塔里木盆地柯坪地区寒武系肖尔布拉克组下段古生产力研究[J]. 中国地质, 45(2): 227−236.

陈践发, 孙省利. 2004. 华北新元古界下马岭组富有机质层段的地球化学特征及成因初探[J]. 天然气地球科学, 15(2):110−114.

陈孝红, 危凯, 张保民, 李培军, 李海, 刘安, 罗胜元. 2018. 湖北宜昌寒武系水井沱组页岩气藏主控地质因素和富集模式[J]. 中国地质, 45(2): 207−226.

方杰, 刘宝泉, 金凤鸣, 刘敬强, 鱼占文. 2002. 华北北部中、上元古界生烃潜力与勘探前景分析[J]. 石油学报, 23(4): 18−23.

郝石生. 1990. 华北北部中—上元古界石油地质学[M]. 东营: 石油大学出版社.

霍勇, 罗顺社, 张建坤, 庞秋维, 金姗姗, 尚飞. 2012. 燕山地区宣龙坳陷中元古界洪水庄组—铁岭组沉积相分析与层序格架的建立[J]. 地质科技情报, 31(3):11−18.

罗顺社, 吕奇奇, 李琳静, 淡卫东. 2012. 燕山地区宣龙坳陷洪水庄组和铁岭组沉积环境[J]. 海洋地质前沿, (2):10−16.

罗情勇, 钟宁宁, 朱雷, 延年, 秦婧, 齐琳, 张毅, 马勇. 2013. 华北北部中元古界洪水庄组埋藏有机碳与古生产力的相关性[J]. 科学通报, (11): 1036−1047.

蓝廷广, 范宏瑞, 胡芳芳, 等. 2012. 鲁东昌邑古元古代 BIF 铁矿矿床地球化学特征及矿床成因讨论[J]. 岩石学报, 28(11): 167−183.

梅冥相, 李志忠, 河北兴隆中. 1998. 上元古界旋回层序初步研究[J]. 地层学杂志, (2):102−108.

旷红伟, 李家华, 彭楠, 罗顺社, 岑超. 2009. 燕山地区 1.6 ~ 1.0ga 时期碳酸盐岩碳、氧同位素组成、演化及其地质意义[J]. 地学前缘, 16(5):118−133.

李怀坤, 朱士兴, 相振群, 苏文博, 陆松年, 周红英, 耿建珍, 李生, 杨锋杰. 2010. 北京延庆高于庄组凝灰岩的锆石 U−Pb 定年研究及其对华北北部中元古界划分新方案的进一步约束[J]. 岩石学报, 26(7): 2131−2140.

李红中, 周永章, 张连昌, 何俊国, 杨志军, 梁锦, 周留煜, 瓦西拉里. 2012. 华北克拉通南部元古代熊耳群硅质岩地球化学及形成机制研究[J]. 岩石学报, 28(11):3679−3691.

曲永强, 孟庆任, 马收先, 李林, 武国利. 2010. 华北地块北缘中元古界几个重要不整合面的地质特征及构造意义[J]. 地学前缘, 17(4): 112−127.

乔秀夫, 高林志, 张传恒, 2007a. 中朝板块中、新元古界年代地层柱与构造环境新思考[J]. 地质通报, 26(5):503−509.

秦婧, 钟宁宁, 齐雯, 张彦起, 罗情勇. 2010. 华北北部洪水庄组有机岩石学[J]. 石油与天然气地质, 31(3):367−374.

孙省利, 陈践发, 刘文汇, 张水昌. 2003. 海底热水活动与海相富有机质层形成的关系——以华北新元古界青白口系下马岭组为例[J]. 地质论评, 49(6): 588−595.

王浩, 凌文黎, 段瑞春, 杨红梅, 陈子万, 秦雅东. 2012. 扬子克拉通峡东地区新元古代—寒武纪黑色岩系 Os 同位素地球化学特征及其地质意义[J]. 地球科学——中国地质大学学报, 37(3):451−462.

王铁冠, 韩克猷. 2011. 论中—新元古界的原生油气资源[J]. 石油学报, 32(1):1−7.

王杰, 陈践发. 2001. 华北中上元古界烃源岩沉积环境及生烃潜力研究[J]. 天然气地球科学, 12(3):27−33.

吴朝东, 杨承运, 陈其英. 1999. 湘西黑色岩系地球化学特征和成因意义[J]. 岩石矿物学杂志,(1):26−39.

吴因业, 刘伟, 刘艳, 方向, 马奎. 2016. 石油学报. 中国冈瓦纳的寒武系下伏沉积及其石油地质意义[J]. 37(9): 1069−1079.

解启来, 陈多福, 漆亮, 陈先沛. 2003. 贵州瓮安陡山沱组磷块岩的稀土元素地球化学特征与沉积古环境[J]. 矿物学报, 23(4):289−295.

徐勇航. 2010. 华北克拉通南部古元古界熊耳群中海绿石的发现及其地质意义[J]. 沉积学报, 28(4):671−675.

杨世文, 楼法生, 杨坤光, 张芳荣, 凌国卿, 曹员兵. 2016. 江西南部震旦−寒武纪寻乌岩组变沉积岩地球化学特征及构造意义[J]. 中国地质, 43(1):349−364.

于炳松, 裴愉卓. 1998. 贵州地区新元古代—三叠纪沉积岩中稀土元素地球化学特征与地壳演化[J]. 现代地质, 12(2):173−179.

赵文智, 胡素云, 汪泽成, 张水昌, 王铜山. 2018. 中国元古界—寒武系油气地质条件与勘探地位[J]. 石油勘探与开发, 45(1):1−13.